Supporting Information

Management of Perovskite Intermediates for Highly Efficient Inverted Planar Heterojunction Perovskite Solar Cells

Yingdong Xia,[‡a] Chenxin Ran, [‡b] Yonghua Chen,*[a] Qi Li,[c] Naisheng Jiang,[d] Changzhi Li,[e] Yufeng Pan,[a] Taotao Li,[a] JianPu Wang*[a] and Wei Huang*[a]

[a]*Key Laboratory of Flexible Electronics (KLOFE) & Institution of Advanced Materials (IAM), Jiangsu National Synergetic Innovation Center for Advanced Materials (SICAM), Nanjing Tech University (NanjingTech), 30 South Puzhu Road, Nanjing, Jiangsu, 211816, P. R. China*

*Email: iamyhchen@njtech.edu.cn; iamjpwang@njtech.edu.cn; iamwhuang@njtech.edu.cn;

[b]*Electronic Materials Research Laboratory, Key Laboratory of Education Ministry & International Center for Dielectric Research, Xi'an Jiaotong University, Xi'an, Shaanxi 710049, P.R. China*

[c]*Physical Science, IBM TJ Watson Center, Yorktown Heights, NY 10598, USA*

[d]*Department of Materials Science and Engineering, Stony Brook University, Stony Brook, NY 11794-2275, USA*

[e]*MOE Key Laboratory of Macromolecular Synthesis and Functionalization, State Key Laboratory of Silicon Materials, Department of Polymer Science and Engineering, Zhejiang University, Hangzhou 310027, P. R. China*

‡These authors contributed equally to this work.

Experimental Method

Synthesis of methylammonium acetate (MAAc): A acetic acid, glacial (15.3 mL, 0.327 mol, Fisher Scientific) and methylamine (27.8 mL, 0.491 mol, 40% in ethanol, Aldrich) were stirred in a 250 mL round bottom flask in an ice bath for 2 h. After stirring at 0 °C for 2 h, the resulting solution was recovered by rotary evaporation at 80 °C for 1 h and produced synthesized chemicals MAAc. The product was washed three times with diethyl ether and then was dissolved in ethanol, recrystallized from diethyl ether three times, and dried at 60 °C in a vacuum oven for 24 h.

Synthesis of methylammonium iodide (MAI): A hydroiodic acid (30 mL, 0.227 mol, 57 wt.% in water, Aldrich) and methylamine (27.8 mL, 0.273 mol, 40% in ethanol, Aldrich) were stirred in a 250 mL round bottom flask in an ice bath for 2 h. After stirring at 0 °C for 2 h, the resulting solution was recovered by rotary evaporation at 80 °C for 1 h and produced synthesized chemicals MAI. The product was washed three times with diethyl ether and then was dissolved in ethanol, recrystallized from diethyl ether three times, and dried at 60 °C in a vacuum oven for 24 h.

Preparation of perovskite precursor solution: The synthesized MAI (0.159g) and MAAc (0.135g) was mixed with PbI_2 (0.461g) in anhydrous N, N-dimethylformamide by stirring at 60 °C for 30 min to produce a clear perovskite solution. The molar ratio for PbI_2:MAI:MAAc is around 1:1:1.5. Then the solution was cooled down to room temperature. The perovskite solutions with different ratios of MAAc were prepared in a similar manner.

Electronic structure calculation of $MAPbI_{3-x}Ac_x$ perovskite: We focused on β phase $MAPbI_3$ as it is shown to be the dominant phase under room temperature.[S1, S2] The crystal structure is tetragonal, space group I4/mcm (No. 140 of the International Tables of Crystallography). We adopted the MA1 orientation in order to remove the overall shear in the original cell.[S2] Our first principles calculations are carried out in the projector augmented wave (PAW)[S3] framework in the planewave density functional theory (DFT) package QUANTUM-ESPRESSO.[S4] We employ Perdew-Burke-Ernzerhof (PBE) paramatrized generalized gradient approximation (GGA) pseudopotentials.[S5] The kinetic cut-off energy is 500 eV. A self-consistency convergence criterion of $1x10^{-6}$ eV was used for all calculations and all the structures are fully relaxed until all residual force components on any atoms are less than 0.02 eV/Å. The bulk properties of ideal $MAPbI_3$ are calculated with the primitive unit cell of 48 atoms. A Γ-centered 6×6×4 Monkhorst-Pack k-point mesh is applied to

converge the charge densities. Due to the existence of the heavy elements, spin-orbit coupling (SOC) included calculations were also performed and compared with the non-SOC(NSOC) results. The electron/hole effective masses are calculated by

$$m_{e/h}^{*} = \hbar^2 \left[\frac{\partial^2 \varepsilon(k)}{\partial^2 k} \right]^{-1}$$

at the bottom of the conduction band/top of the valance band.

Fabrication of perovskite solar cells: The device is fabricated in the configuration of indium tiin oxide (ITO)/poly(3,4-ethylenedioxythiophene):poly(styrenesulfonate) (PEDOT:PSS)/$CH_3NH_3PbI_3$/[6,6]-phenyl-C61-butyric acid methylester (PCBM)/fullerene surfacant (FPI-PEIE)/Ag. ITO glass substrates were cleaned sequentially with detergent, de-ionized water, acetone, and *iso*-propanol, followed by drying with N_2 flow and UV-ozone treatment for 15 minutes. The PEDOT:PSS solution (Al4083 from H. C. Starck) was spin-cast onto ITO electrodes at 5000 rpm for 40 s, followed by heating at 140 °C for 10 minutes. The PEDOT:PSS-coated ITO/Glass substrate was then transferred to an Ar-filled glovebox for perovskite film fabrication. The substrate was first heated to a desired temperature (60 °C-100 ºC) and the perovskite precursor solution with PbI_2, MAI, and MAAc was always kept at room temperature. To deposit perovskite films, the perovskite precursor solution (40 μL) was first quickly dropped onto a preheated PEDOT:PSS-coated ITO/Glass substrate. The substrate was then spun immediately at 5000 rpm for 30 s. The spin coater is programed to reach a speed of 5000 rpm in 1 second in order to prevent the temperature from quenching. This instantly changed the color of the substrate from transparent to light brown after spin coating for several seconds depending on the substrate temperature and the ratio of MAAc in the precursor. The formed perovskite was then thermally annealed at 100 °C for 1 minute in the glovebox to complete crystallization of the perovskite. After the annealing, PCBM in chlorobenzene solution (25 mg ml^{-1}) and FPI-PEIE (2 mg mL^{-1} in methanol) were sequentially deposited onto the perovskite layer at 1000 rpm for 60 s and 3000 rpm for 30 s respectively. Finally, the device was transferred to the evaporator for thermal evaporation of Ag (100 nm) at a pressure of 10^{-7} Torr. The area of each device is 0.1 cm^2, as defined by the overlap of the ITO and the thermally evaporated Al.

Electrical, Optical, and Microscopic Characterization of Films and Devices: All measurements were carried out under ambient conditions. Scanning electron microscopic (SEM) images were taken on a Nova nanoSEM 600. UV/Vis absorption was measured with a Shimadzu UV1800 spectrometer. X-ray diffraction (XRD) was performed with a Rigaku MiniFlexII XRD system. Fourier transform infrared spectra (FITR) were recorded on a PerkinElmer spectrum GX FTIR unit. Atomic force microscopy (AFM) images were performed on an Agilent 5500 atomic force microscope. Thermal decomposition profiles were recorded by a thermogravimetric analyzer (TGA) TA Q50 in nitrogen atmosphere with a flow rate of 20 ml min^{-1}. The temperature varied from 25 to 600 °C at a heating rate of 10 °C min^{-1}. Film thickness was measured by a KLA-Tencor P-6 Stylus profilometer.

Characterization of perovskite solar cells: All the devices were tested in an Ar-filled glovebox using a Keithley 2400 source meter and a Newport Oriel sol 2A solar simulator (300 W). The light intensity was calibrated to be 100 mW cm^{-2} using a calibrated Si solar cell and a KG5 color filter. The device performance parameters were obtained from the current-voltage curves of the perovskite solar cells under illumination. The incident photon-to-current efficiency **(**IPCE) was measured on a Solar Cell Measurement System from PV measurement Inc. We used the 91150V Reference Cell and Meter (ORIEL instrument) to calibrate the light intensity prior to the device testing.

Supporting Table S1. PBE calculated lattice constants in Å, band gaps in eV, and effective masses in electron mass (m_0) of $MAPbI_{3-x}Ac_x$. Note that in the single site replacement case, the lattice is kept unchanged.

x	Lattice constant (Å)		Band gap (eV)		m_e^* (m_0)			m_h^*(m_0)		
	a	c	NSOC	SOC	x/y	z	average	x/y	z	average
0	9.00	12.90	1.73	0.69	0.19	0.16	0.18	0.28	0.23	0.27
0.25	-	-	1.84	0.77	0.23	1.12	0.53	0.25	0.40	0.30
3	9.63	14.31	2.82	1.80	0.46	0.88	0.60	0.34	0.27	0.32

Supporting Table S2. RMS roughness of $MAPbI_3$ perovskite formed at different substrate temperatures and different ratios of MAAc based on the images shown in Figure 3b and 3d.

	ST	60 °C	80 °C	100 °C	1:1:1	1:1:1.5	1:1:2	1:1:3
RMS (nm)	42.2	13.4	18.4	30.9	44.8	18.4	28.7	56.6

Supporting Table S3. The top device performance in planar-heterojunction structure with organic charge transporting layers.

Structures	V_{oc} (V)	J_{sc} (mA cm^{-2})	FF	PCE (%)	Refs.
ITO/PEDOT:PSS/$MAPbI_3$/PCBM/FPI-PEIE/Ag	**1.00**	**22.90**	**0.79**	**18.09**	**This work**
ITO/PEDOT:PSS/$MAPbI_3$/PCBM/Au	1.10	20.90	0.79	18.10	S6
ITO/PEDOT:PSS/$MAPbI_{3-x}Cl_x$/PCBM/Al	0.94	22.40	0.83	17.48	S7
ITO/PEDOT:PSS/$MAPbI_3$/PCBM/BCP/Ag	1.00	22.34	0.82	18.32	S8

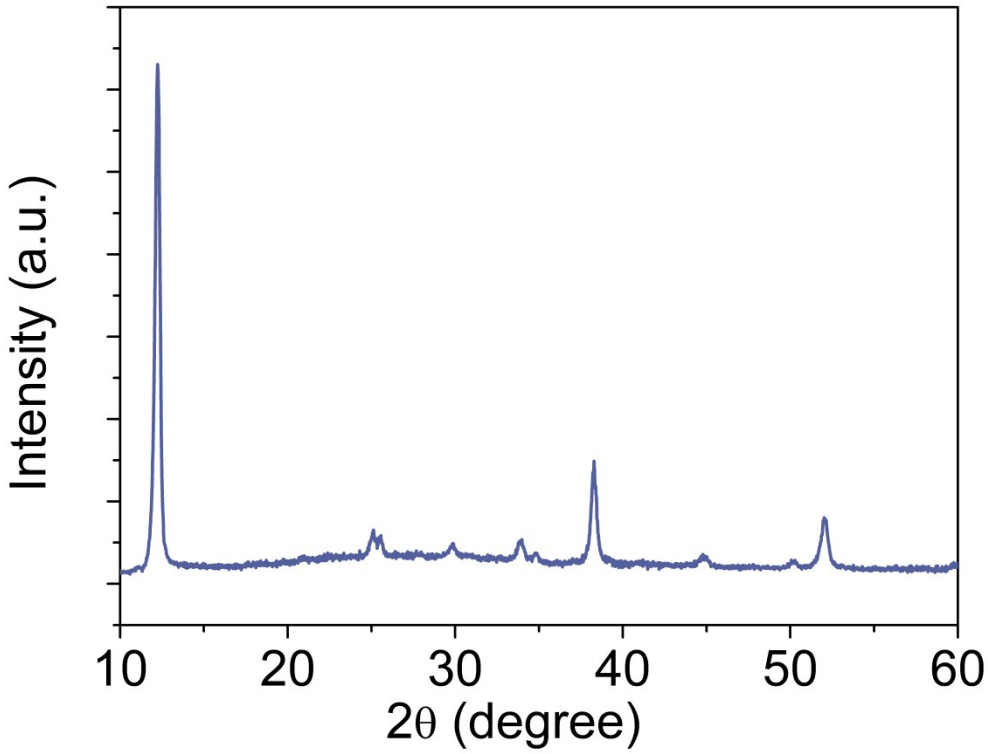

Figure S1. XRD patterns of PbI_2 film on ITO/PEDOT:PSS substrate.

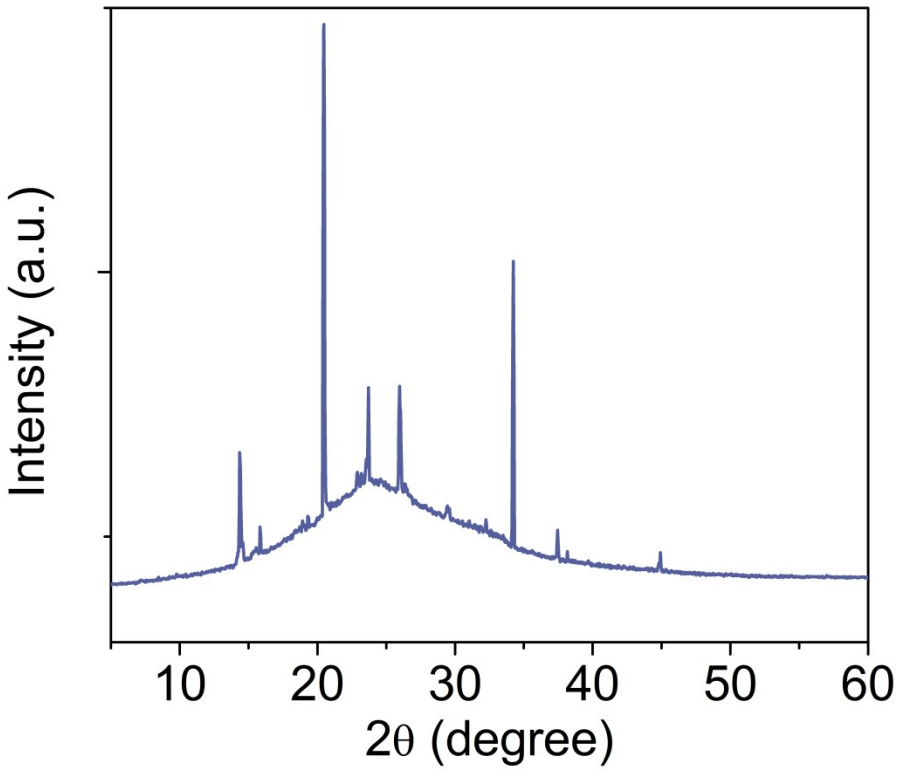

Figure S2. XRD patterns of MAAc powder.

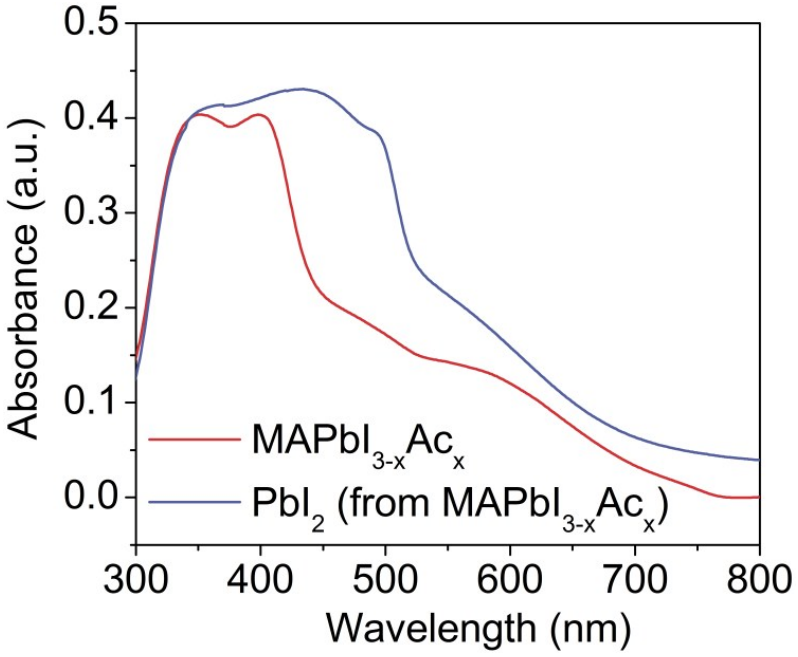

Figure S3. Absorption of $MAPbI_{3-x}Ac_x$ perovskite and PbI_2 from $MAPbI_{3-x}Ac_x$ perovskite decomposition.

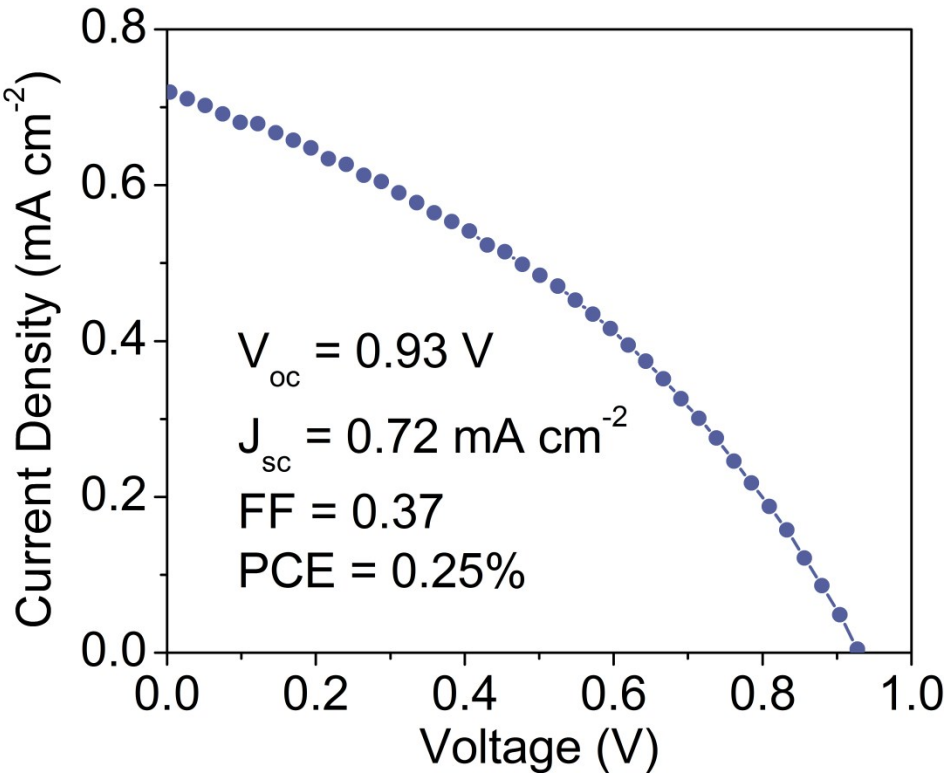

Figure S4. *J-V* curve of device based on $MAPbI_{3-x}Ac_x$ perovskite. The device structure is ITO/PEDOT:PSS/$MAPbI_{3-x}Ac_x$/PCBM/FPI-PEIE/Ag. The open-circuit voltage (V_{oc}), short-circuit current density (J_{sc}), fill factor (FF), and PCE were determined as 0.93 V, 0.72 mA cm^{-2}, 0.37, and 0.25%, respectively.

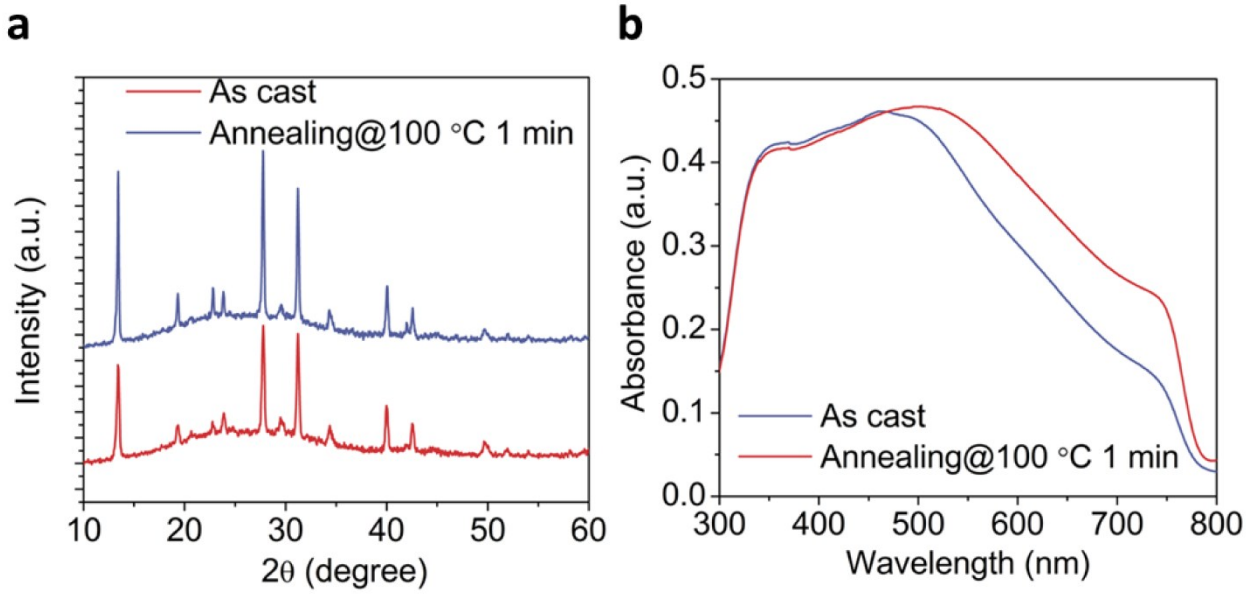

Figure S5. a, **XRD patterns and b, absorption spectra of $MAPbI_3$ from as-cast film and annealing film.** The diffraction peaks and the absorption at longer wavelength are enhanced after annealing due to the further crystallization.

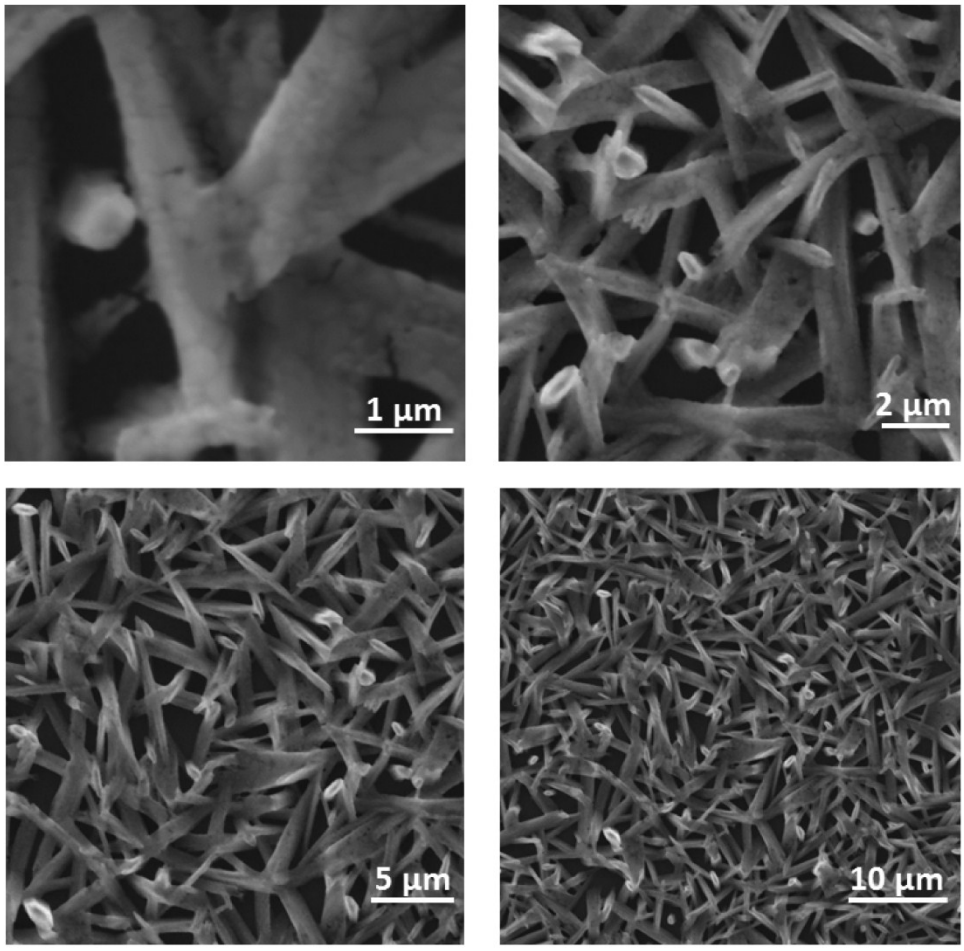

Figure S6. SEM images of $MAPbI_3$ perovskite obtained from PbI_2·MAI precursor without MAAc. The resulting morphology from PbI_2·MAI precursor without MAAc appears as inhomogeneous needle-like structure with low coverage on the substrate.[S13]

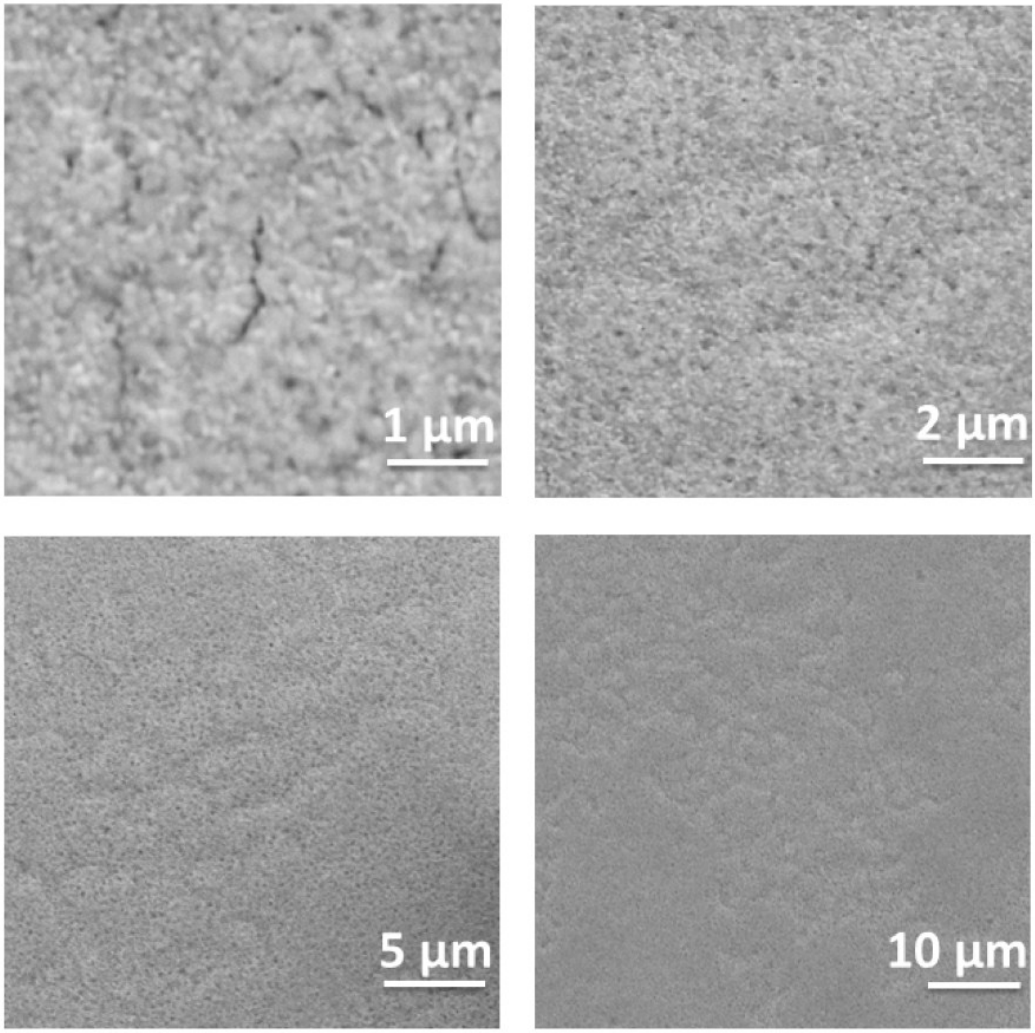

Figure S7. SEM images of $MAPbI_3$ perovskite made from $Pb(Ac)_2$ as a lead source using the same spin-coating procedure. The solution was prepared by mixture of $Pb(Ac)_2$ and MAI as a molar ratio of 1:3.[S14] The ITO/PEDOT:PSS substrate temperature was kept at 80 °C before spin-coating at 5000 rpm for 30 s.

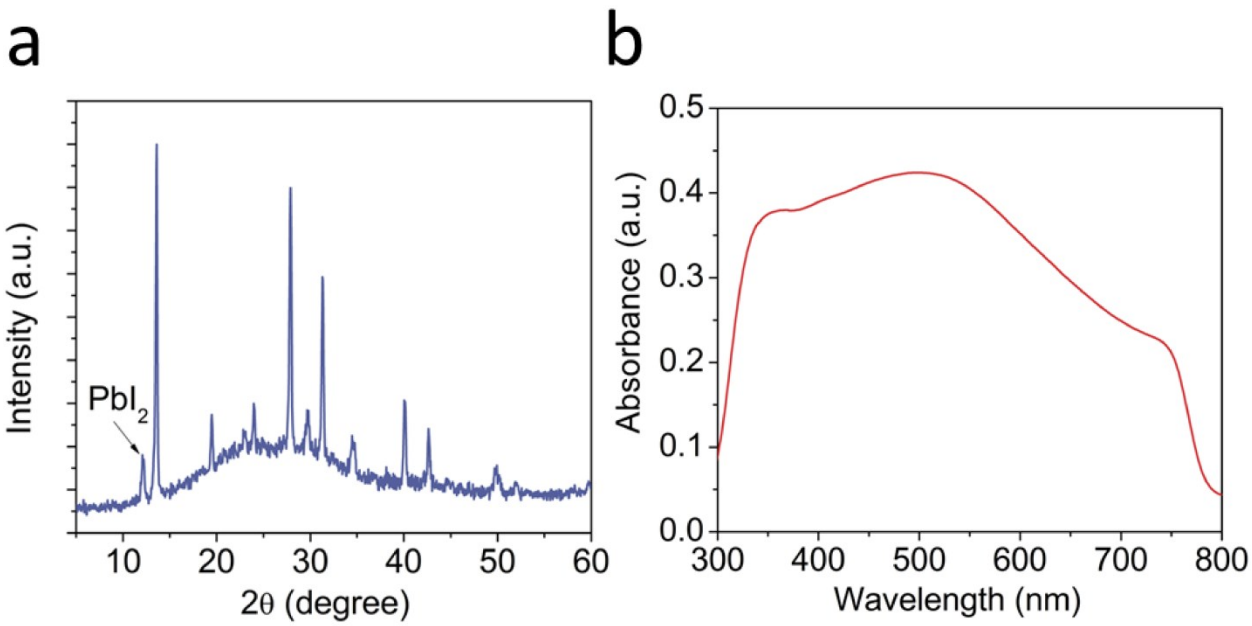

Figure S8. a, XRD pattern and b, absorption spectrum of $MAPbI_3$ perovskite made from $Pb(Ac)_2$. The PbI_2 peak can be clearly seen, demonstrating the incomplete transformation from $Pb(Ac)_2$ to $MAPbI_3$ perovskite.

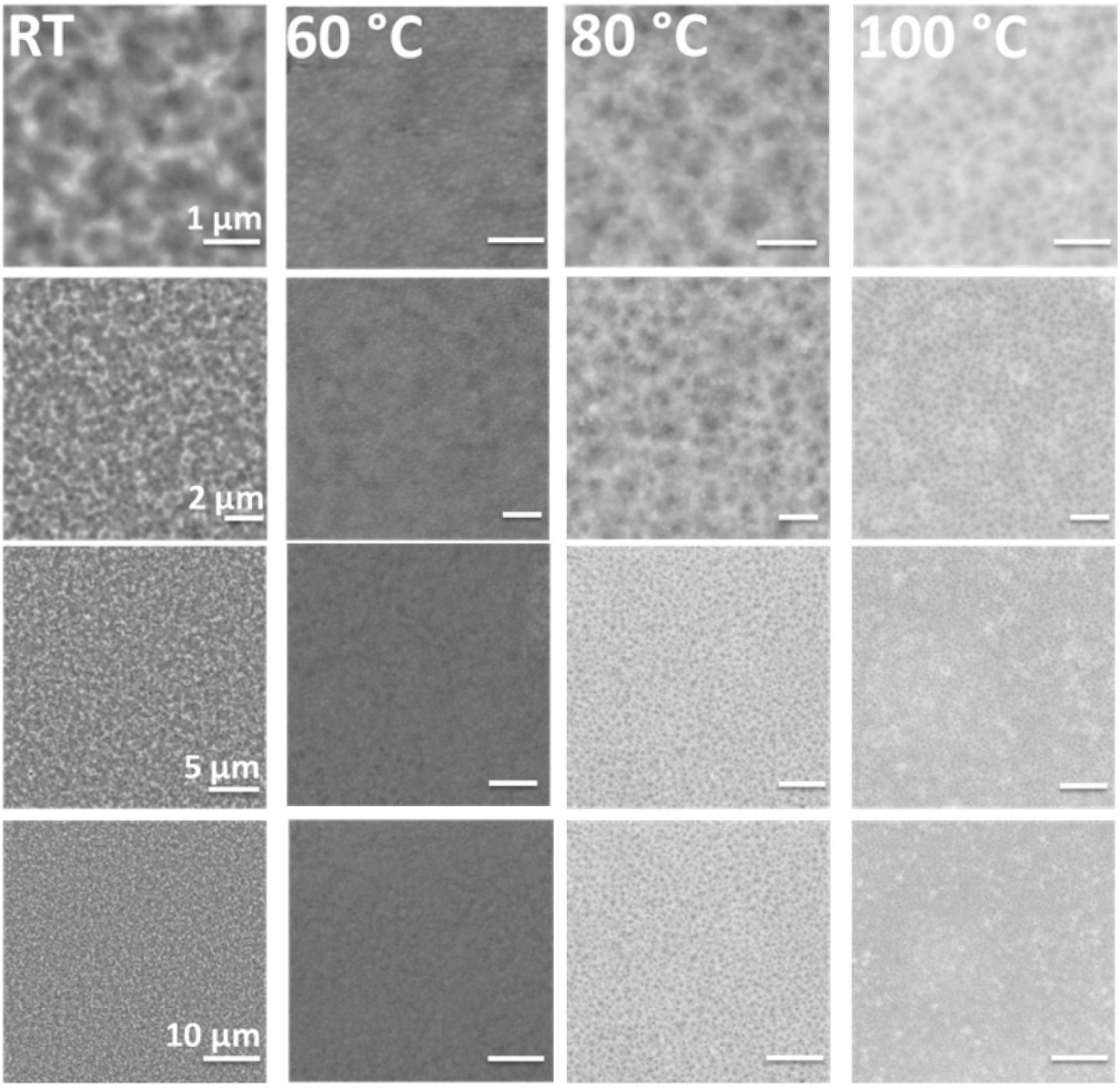

Figure S9. SEM images of formed $MAPbI_3$ perovskite with different magnification at different substrate temperatures. The nanoscale holes are gradually formed with increasing temperature.

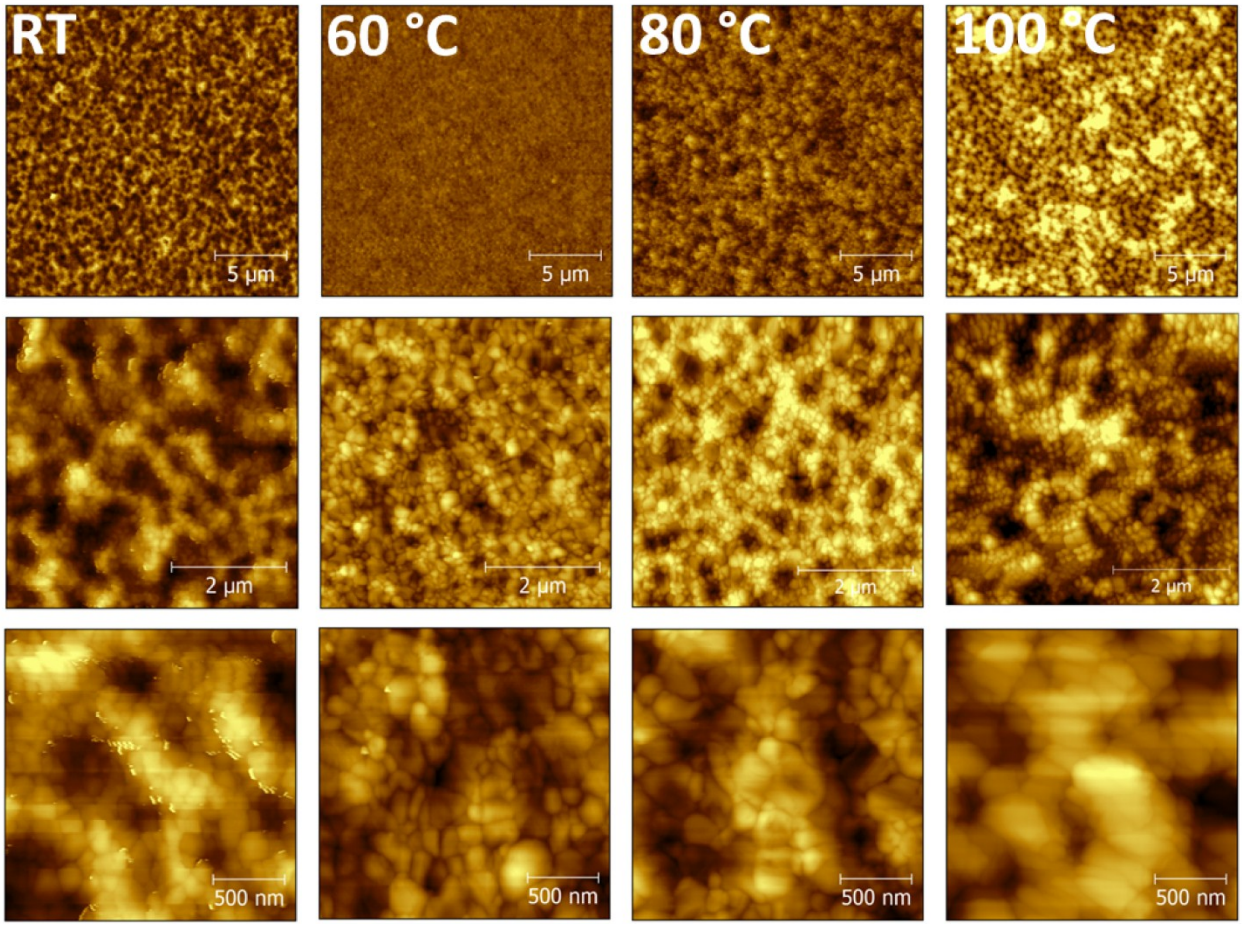

Figure S10. AFM images of $MAPbI_3$ perovskite formed at different substrate temperatures with different magnification.

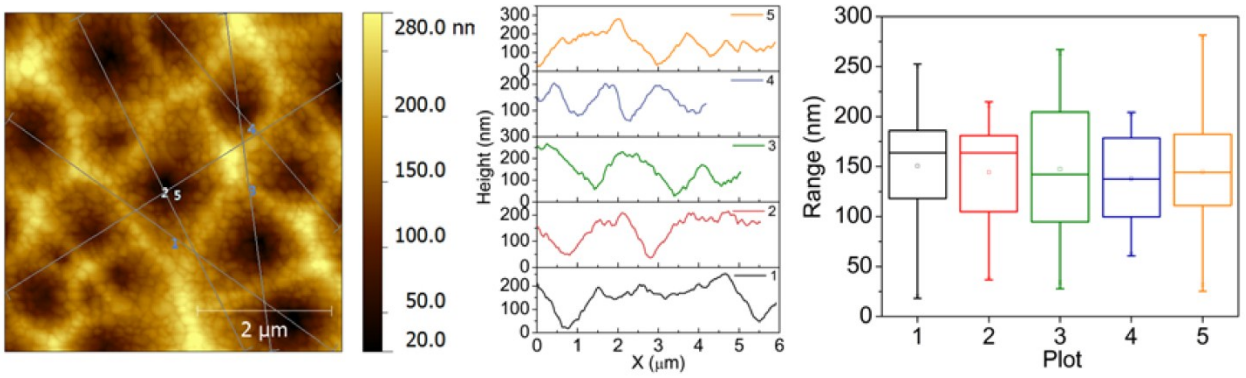

Figure S11. AFM image of $MAPbI_3$ perovskite formed at a substrate temperature of 120 °C.

The RMS roughness of the image is 59 nm. The average depth of holes is around 150 nm.

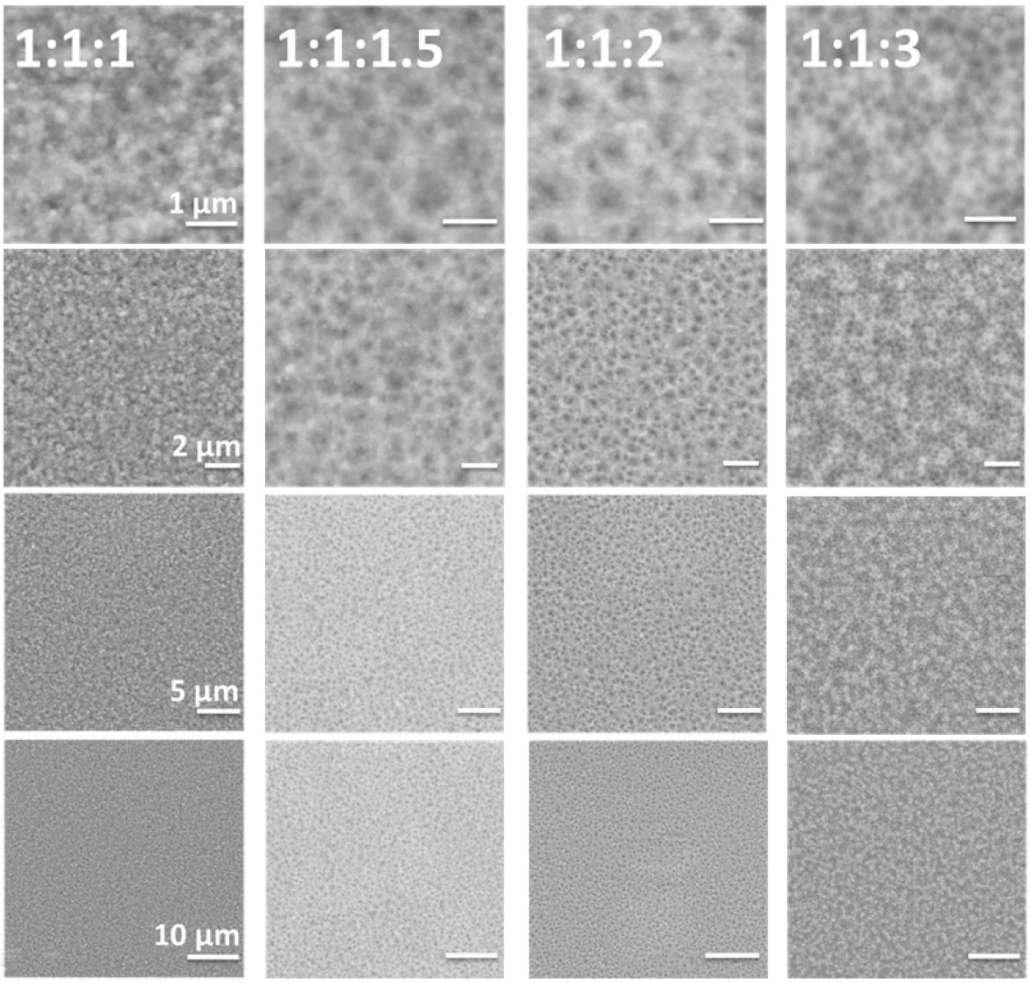

Figure S12. SEM images of $MAPbI_3$ perovskite formed at different ratios of MAAc with different magnification.

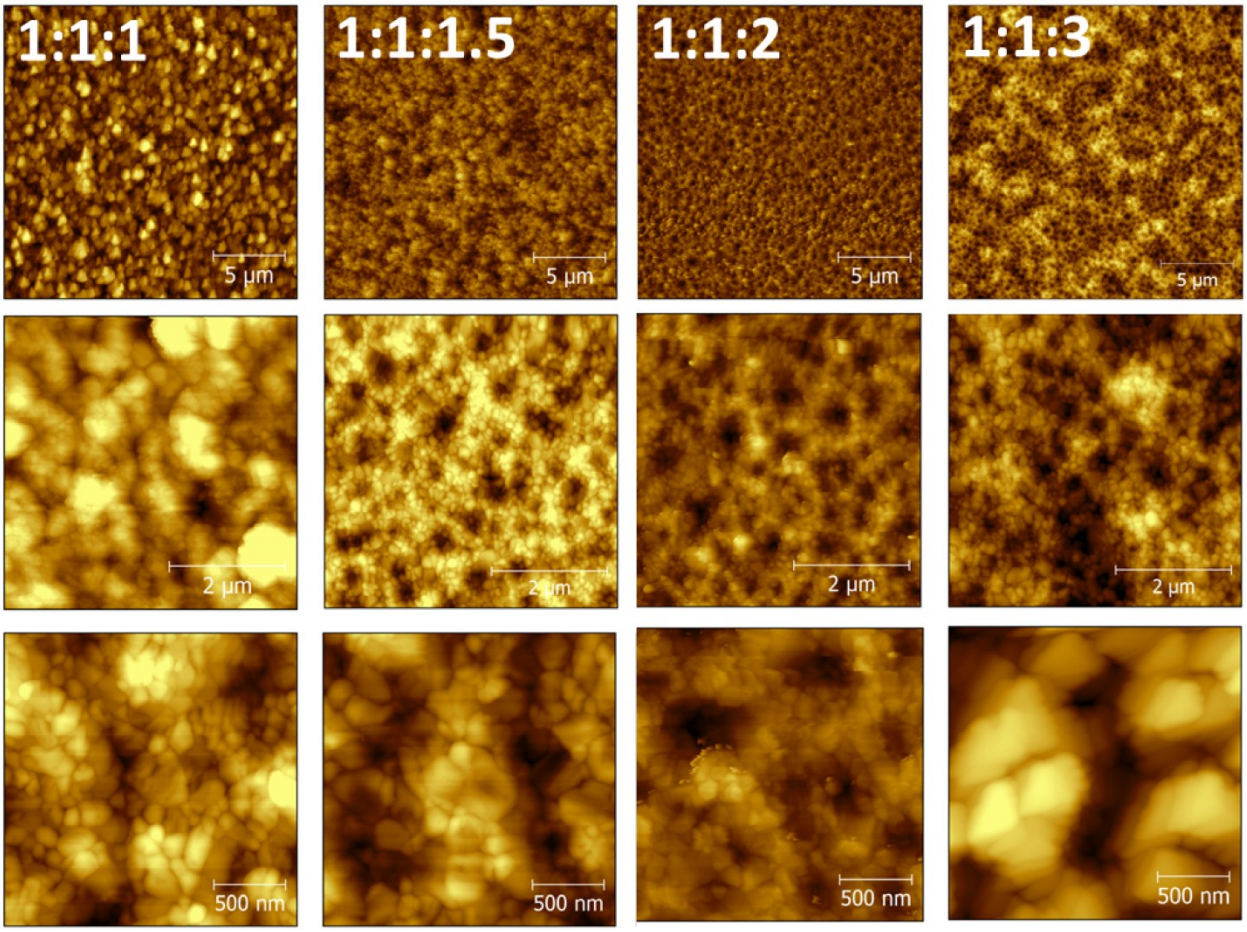

Figure S13. AFM images of $MAPbI_3$ perovskite formed at different ratios of MAAc with different magnification.

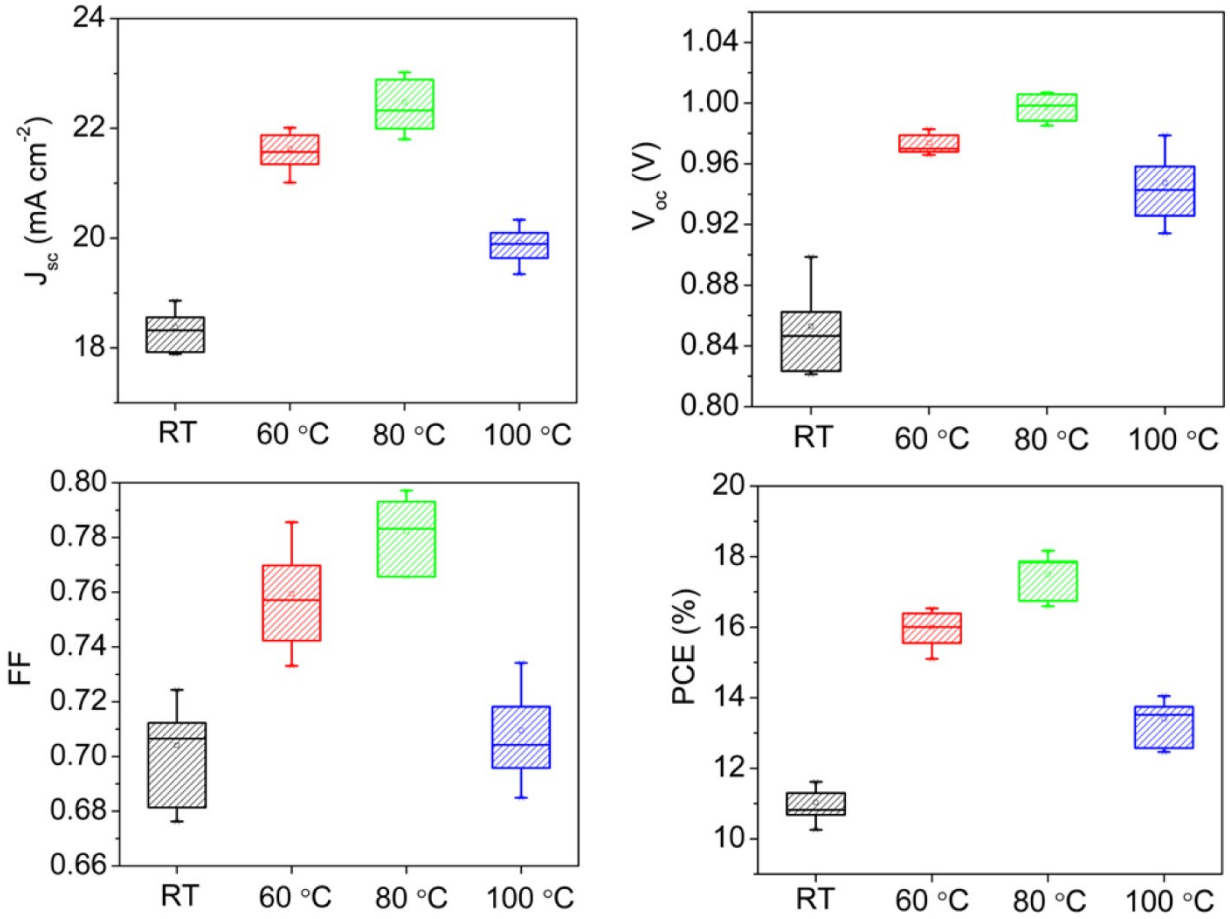

Figure S14. Short-circuit current density (J_{sc}), open-circuit voltage (V_{oc}), fill factor (FF) and power conversion efficiency (PCE) versus substrate temperature. Error bars represents minimum and maximum values, and the middle line in each box represents the median value. Filled squares indicate mean values.

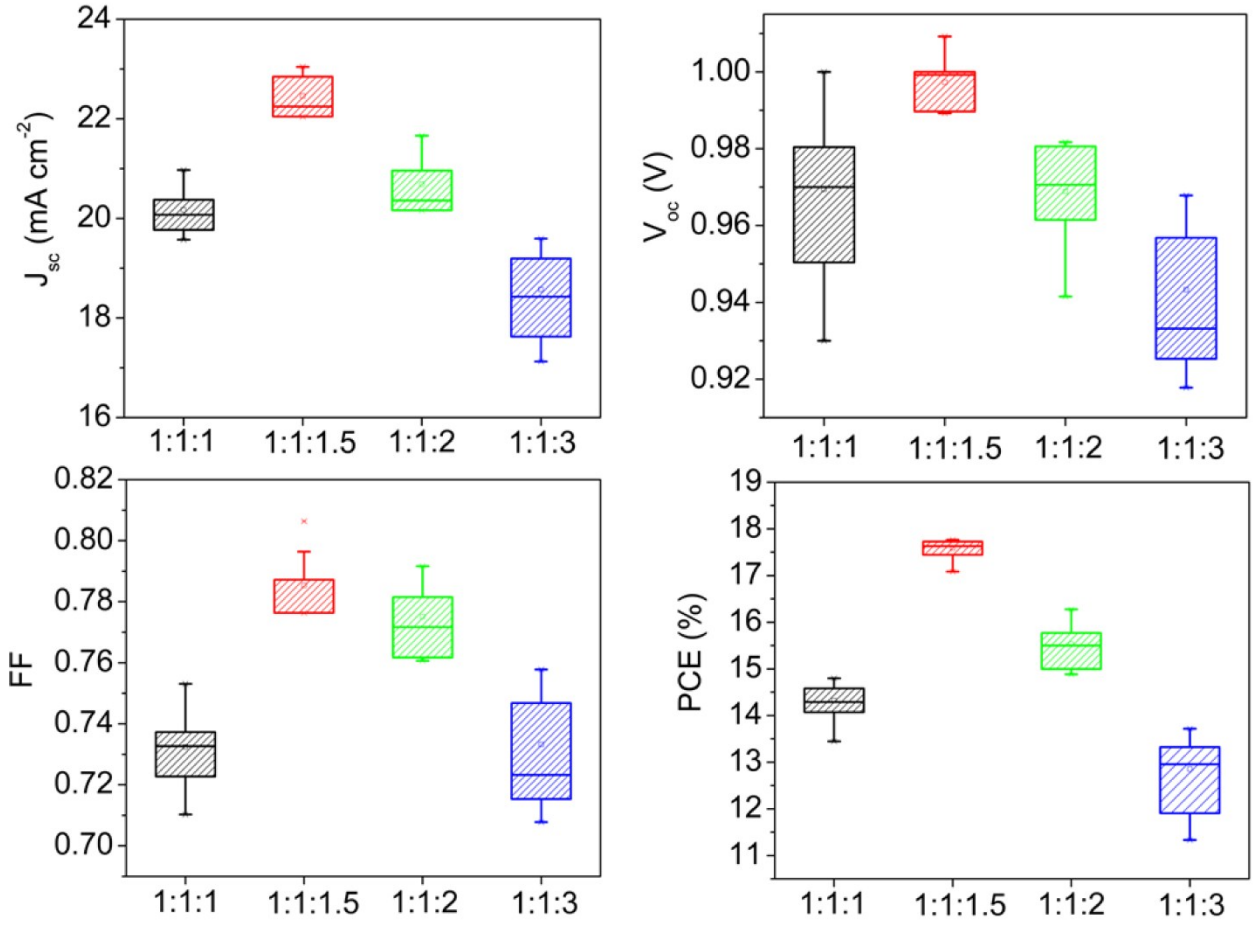

Figure S15. Short-circuit current density (J_{sc}), open-circuit voltage (V_{oc}), fill factor (FF) and power conversion efficiency (PCE) versus MAAc ratio. Error bars represents minimum and maximum values, and the middle line in each box represents the median value. Filled squares indicate mean values.

Supporting References

S1. W.-J. Yin, J.-H. Yang, J. Kang, Y. Yan, S.-H. Wei, *J. Mater. Chem. A* **2015,** *3,* 8926.

S2. F. Zheng, H. Takenaka, F. Wang, N. Z. Koocher, A. M. Rappe, *J. Phys. Chem. Lett.* **2015,** *6,* 31.

S3. P. E. Blöchl, *Phys. Rev. B* **1994,** *50,* 17953.

S4. P. Giannozzi, *J. Phys.: Condens. Matter.* **2009,** *21,* 395502.

S5. J. P. Perdew, K. Burke, M. Ernzerhof, *Phys. Rev. Lett.* **1996,** *77,* 3865.

S6. J. H. Heo, H. J. Han, D. Kim, T. K. Ahn, S. H. Im, *Energy Environ. Sci.*, **2015**, 8, 1602.

S7. W. Nie, H. Tsai, R. Asadpour, J.-C. Blancon, A. J. Neukirch, G. Gupta, J. J. Crochet, M. Chhowalla, S. Tretiak, M. A. Alam, H.-L. Wang, A. D. Mohite, *Science* **2015,** *347,* 522.

S8. L. Zhao, D. Luo, J. Wu, Q. Hu, W. Zhang, K. Chen, T. Liu, Y. Liu, Y. Zhang, F. Liu, T. P. Russell, H. J. Snaith, R. Zhu, Q. Gong, *Adv. Funct. Mater.* **2016,** *26,* 3508.